MOLECULAR AND CELLULAR BIOLOGY, Mar. 2001, p. 1841–1853 Vol. 21, No. 5
0270-7306/01/$04.00+0 DOI: 10.1128/MCB.21.5.1841–1853.2001

Histone Folds Mediate Selective Heterodimerization of Yeast $TAF_{II}25$ with TFIID Components $yTAF_{II}47$ and $yTAF_{II}65$ and with SAGA Component ySPT7

YANN-GAËL GANGLOFF,[1] STEVEN L. SANDERS,[2] CHRISTOPHE ROMIER,[1] DORIS KIRSCHNER,[1] P. ANTHONY WEIL,[2] LASZLO TORA,[1] AND IRWIN DAVIDSON[1]*

Institut de Génétique et de Biologie Moléculaire et Cellulaire, CNRS/INSERM/ULP, Illkirch Cédex, C.U. de Strasbourg, France,[1] and Department of Molecular Physiology and Biophysics, Vanderbilt University School of Medicine, Nashville, Tennessee 37232[2]

Received 25 August 2000/Returned for modification 30 September 2000/Accepted 7 December 2000

We show that the yeast TFIID (yTFIID) component $yTAF_{II}47$ contains a histone fold domain (HFD) with homology to that previously described for $hTAF_{II}135$. Complementation in vivo indicates that the $yTAF_{II}47$ HFD is necessary and sufficient for vegetative growth. Mutation of highly conserved residues in the α1 helix of the $yTAF_{II}47$ HFD results in a temperature-sensitive phenotype which can be suppressed by overexpression of $yTAF_{II}25$, as well as by $yTAF_{II}40$, $yTAF_{II}19$, and $yTAF_{II}60$. In yeast two-hybrid and bacterial coexpression assays, the $yTAF_{II}47$ HFD selectively heterodimerizes with $yTAF_{II}25$, which we show contains an HFD with homology to the $hTAF_{II}28$ family We additionally demonstrate that $yTAF_{II}65$ contains a functional HFD which also selectively heterodimerizes with $yTAF_{II}25$. These results reveal the existence of two novel histone-like pairs in yTFIID. The physical and genetic interactions described here show that the histone-like $yTAF_{II}$s are organized in at least two substructures within TFIID rather than in a single octamer-like structure as previously suggested. Furthermore, our results indicate that ySPT7 has an HFD homologous to that of $yTAF_{II}47$ which selectively heterodimerizes with $yTAF_{II}25$, defining a novel histone-like pair in the SAGA complex.

Transcription factor TFIID, one of the general factors required for accurate and regulated initiation by RNA polymerase II, comprises the TATA binding protein and TATA binding protein-associated factors (TAF_{II}s) (4, 15). The cDNAs encoding many human TAF_{II}s ($hTAF_{II}$s) have been isolated, revealing a striking sequence conservation with yeast TAF_{II}s ($yTAF_{II}$s) and *Drosophila* TAF_{II}s ($dTAF_{II}$s). A subset of TAF_{II}s are present not only in TFIID but also in the SAGA, PCAF, STAGA, and TFTC complexes (7, 13, 23, 27, 36).

Genetic studies with yeast have shown that TAF_{II}s play an important role in transcriptional regulation of many genes (14). Temperature-sensitive mutations in $yTAF_{II}145$ and $yTAF_{II}90$ result in cell cycle arrest and lethality, but the expression of only a small number of genes is affected (3, 35). In contrast, tight temperature-sensitive mutations in $yTAF_{II}17$, $yTAF_{II}25$, $yTAF_{II}60$, and $yTAF_{II}61/68$, which are present in the TFIID and SAGA complexes, or in the TFIID-specific $yTAF_{II}40$ have a more dramatic effect, the transcription of the majority of yeast genes being affected (2, 21, 24–26, 29).

Initial sequence alignments indicated that $hTAF_{II}80$ (corresponding to $dTAF_{II}60$ and $yTAF_{II}60$), $hTAF_{II}31$ ($dTAF_{II}40$ and $yTAF_{II}17$), and $hTAF_{II}20$ ($dTAF_{II}30\alpha$ and $yTAF_{II}61/68$) presented obvious sequence similarity to histones H4, H3, and H2B, respectively (17, 20). Structural studies show that $dTAF_{II}60$ and $dTAF_{II}40$ interact via a histone fold and form an H3-H4-like heterotetramer (37). These findings, together with biochemical experiments and genetic interaction data obtained with yeasts, led to the proposal that TFIID and the other TAF_{II}-containing complexes contain a histone octamer-like substructure composed of an $hTAF_{II}80$-$hTAF_{II}31$ heterotetramer and two $hTAF_{II}20$ homodimers (8, 16).

Subsequent data show this model to be an oversimplification. $hTAF_{II}28$ and $hTAF_{II}18$ are also histone-like, since they interact via a histone fold domain (HFD) to form a heterodimer (5). The SAGA, PCAF, TFTC, and STAGA component SPT3 shows extensive sequence homology to the HFDs of both $hTAF_{II}18$ and $hTAF_{II}28$ in its N- and C-terminal regions, respectively, and could potentially form a histone-like pair by intramolecular interactions. Contrary to what was first suggested, $hTAF_{II}20$ does not homodimerize but rather heterodimerizes with $hTAF_{II}135$ (10). In yeasts, the $hTAF_{II}20$ homologue $yTAF_{II}68$ heterodimerizes with the SAGA component yADA1, and it has been suggested that $yTAF_{II}68$ may also heterodimerize with $yTAF_{II}48$, a potential homologue of $hTAF_{II}135$, in yTFIID (28, 30). These results indicate that there are many more histone-like pairs in TFIID and SAGA than originally suspected. Recent electron microscopy studies show that TFIID comprises three or four lobes arranged in a horseshoe fashion around a central groove (1, 6). Within the present limits of resolution it appears that no single lobe of TFIID would be big enough to harbor all the known histone fold TAF_{II}s, suggesting that they are shared among two or more of the lobes.

We previously reported that $hTAF_{II}135$ contained an HFD with significant sequence homology to the SAGA component yADA1 (10). Now we show that the $hTAF_{II}135$ HFD also shares significant sequence homology with an HFD in $yTAF_{II}47$ (34). In complementation experiments, the $yTAF_{II}47$ HFD is necessary and sufficient for vegetative yeast growth. The tem-

* Corresponding author. Mailing address: Institut de Génétique et de Biologie Moléculaire et Cellulaire, CNRS/INSERM/ULP, B.P. 163, 67404 Illkirch Cédex, C.U. de Strasbourg, France. Phone: 33 3 88 65 34 40 (45). Fax: 33 3 88 65 32 01. E-mail: irwin@titus.u-strasbg.fr.

perature-sensitive phenotype of a mutation in the yTAF$_{II}$47 HFD can be rescued by overexpression of yTAF$_{II}$25 and, at less restrictive temperatures, by yTAF$_{II}$60, yTAF$_{II}$40, and yTAF$_{II}$19. In yeast two-hybrid and bacterial coexpression experiments, the yTAF$_{II}$47 HFD mediates selective heterodimerization with the conserved core domain of yTAF$_{II}$25. There are therefore both genetic and physical interactions between these two yTAF$_{II}$s, suggesting that they form an additional histone-like pair in yTFIID. Consistent with this idea, we show the conserved core domain of yTAF$_{II}$25 to be an HFD which shares homology with the HFD of the hTAF$_{II}$28 family.

Recently, yTAF$_{II}$65 was identified as a novel component of yTFIID (30). Now we demonstrate that yTAF$_{II}$65 contains an HFD with homology to that of yTAF$_{II}$17, dTAF$_{II}$40, and hTAF$_{II}$31. In contrast to the HFD of yTAF$_{II}$47, the yTAF$_{II}$65 HFD is not sufficient for growth. Nevertheless, deletion or mutation of this domain results in temperature sensitivity, showing that it is important for yTAF$_{II}$65 function. Surprisingly, the yTAF$_{II}$65 HFD also selectively heterodimerizes with yTAF$_{II}$25, which thus has two heterodimerization partners in TFIID.

Finally, as yTAF$_{II}$47 and yTAF$_{II}$65 are not present in SAGA, we sought a heterodimerization partner for yTAF$_{II}$25 in this complex. Our results indicate that ySPT7 contains an HFD with homology to that of yTAF$_{II}$47. This domain mediates selective heterodimerization with yTAF$_{II}$25. Together our results reveal the existence of novel histone-like pairs in the TFIID and SAGA complexes. They highlight the important functional and structural role played by this motif in these complexes and provide evidence that the histone-like yTAF$_{II}$s assemble into at least two distinct substructures within TFIID.

MATERIALS AND METHODS

Yeast strains. The yeast strains used in this study are YSLS67 (*Mat***a** *ura3-1 leu2-3,112 trp1-1 his3-11,15 ade2-11 can1-100 taf47Δhisg-hisg* [pRS416-TAF47]), YSLS67/47 (*MAT***a** *ura3-1 leu2-3,112 trp1-1 his3-11,15 ade2-11 can1-100 taf47Δhisg-hisg* [pAS3-TAF47)], YSLS67/47HFD (*MAT***a** *ura3-1 leu2-3,112 trp1-1 his3-11,15 ade2-11 can1-100 taf47Δhisg-hisg* [pAS3-TAF47(1–81)]), YSLS67/47m1 (*MAT***a** *ura3-1 leu2-3,112 trp1-1 his3-11,15 ade2-11 can1-100 taf47Δhisg-hisg* [pAS3-TAF47(R13D, I14E)]), YSLS67/VP16AD47HFD (*MAT***a** *ura3-1 leu2-3,112 trp1-1 his3-11,15 ade2-11 can1-100 taf47Δhisg-hisg* [pASV3-TAF47(1–81)]), YSLS58 (*MAT***a** *ura3Δ0 leu2Δ0 his3Δ1 lys2Δ0 MET15 KAN Δtaf65* [pRS416-TAF65]), YSLS58/65 (*MAT***a** *ura3Δ0 leu2Δ0 his3Δ1 lys2Δ0* MET15 KAN *Δtaf65* [pAS3-TAF65]), YSLS58/65ΔHFD (*MAT***a** *ura3Δ0 leu2Δ0 his3Δ1 lys2Δ0 MET15 KAN Δtaf65* [pAS3-TAF65(103–510)]), YSLS58/65m1 (*MAT***a** *ura3Δ0 leu2Δ0 his3Δ1 lys2Δ0 MET15 KAN Δtaf65* [pAS3-TAF65(L64P, L67P)]), YSLS58/VP16AD65 (*MAT***a** *ura3Δ0 leu2Δ0 his3Δ1 lys2Δ0 MET15 KAN Δtaf65* [pASV3-TAF65]), and L40 [*MAT***a** *trp1-901 leu2-3,112 his3-Δ200 ade2 LYS2*::(LexAop)$_4$-*HIS3 URA3*::(LexAop)$_8$-Lac].

Construction of recombinant plasmids. All yeast and bacterial expression vectors were constructed by PCR using primers with the appropriate restriction sites, and constructs were verified by automated DNA sequencing. Details of constructions are available on request. LexA fusions were constructed in the multicopy vector pBTM116 containing the *TRP1* marker, and the VP16 fusions were constructed in the multicopy vector pASV3 containing the *LEU2* marker (10). For complementation, wild-type or mutated yTAF$_{II}$s were cloned in the multicopy pAS3 plasmid with a *LEU*$^-$ marker.

Two-hybrid, complementation, and high-copy-number temperature-sensitive suppression assays. All yeast strains were transformed by the lithium acetate technique. For two-hybrid assays, transformants were selected on Trp$^-$ Leu$^-$ plates. Quantitative β-galactosidase assays on individual L40 transformants were determined as previously described (10). Reproducible results were obtained in several independent experiments, and the results of a typical experiment are shown in the figures. Yeast strains YSLS67 and YSLS58, used for plasmid shuffling of *TAF47* and *TAF65*, were derived from YJR10 (34) and YSLS41 (30) by sporulation and tetrad dissection. For complementation assays, the rescue plasmids indicated in the relevant figures were transformed and the wild-type *TAF*/*URA3* plasmid was shuffled out by two passes on media containing 5-fluoroorotic acid. For suppression of the yTAF$_{II}$47(R13D, I14E) mutant strain, cells were transformed with high-copy-number plasmids with a *URA3* marker expressing the indicated yTAF$_{II}$s and serial dilutions of the transformants were spotted at 30, 34, and 36°C. Plates at the restrictive temperatures were photographed after 3 days of growth. In all experiments cultures were grown in yeast extract-peptone-dextrose unless selection was necessary, in which case all cultures were grown in the appropriate selective synthetic dextrose (SD) medium.

Coexpression in *Escherichia coli*. Coexpression in *E. coli* was performed as previously described (9a, 10). All plasmids were constructed by PCR, and details are available on request. The yTAF$_{II}$47, yTAF$_{II}$65, and SPT7 histone fold regions were expressed as glutathione *S*-transferase (GST) fusion proteins in pGEX2T. Native untagged, yTAF$_{II}$25, hTAF$_{II}$30, and yTAF$_{II}$68 HFDs were expressed from a modified version of the vector pACYC184 (New England Biolabs). Plasmids pairs were introduced into *E. coli* strain BL21(DE3), and double transformants were selected on plates containing ampicillin and chloramphenicol. Bacteria were amplified to an optical density at 600 nm of 0.45 and induced for 4 h at 25°C with 1 mM isopropyl-β-D-thiogalactopyranoside (IPTG). Cell were lysed by sonication in buffer (25 mM Tris-HCl [pH 6.0] and 0.4 M NaCl), and the soluble fraction was collected after centrifugation at 14,000 rpm for 20 min at 4°C in an Eppendorf centrifuge. Aliquots of the soluble fraction from a 10-ml bacterial culture were then incubated with glutathione-Sepharose (Pharmacia). Binding and washing were done essentially as described previously (10). Bound proteins were analyzed by sodium dodecyl sulfate-polyacrylamide gel electrophoresis and staining with Coomassie brilliant blue.

RESULTS

yTAF$_{II}$47 contains an HFD which suffices for vegetative growth. Previously we reported that hTAF$_{II}$135 amino acids 870 to 944 showed significant sequence homology to H2A, NC2α and yADA1 (10) (Fig. 1). The hTAF$_{II}$135 HFD also shows significant homology to yTAF$_{II}$48, the hTAF$_{II}$135 homologue in yTFIID (28, 30) (Fig. 1). Database searches also revealed a significant similarity between the HFD of the TAF$_{II}$135 family and the N-terminal region of yTAF$_{II}$47 (Fig. 1). In the yTAF$_{II}$47 HFD, the conserved RI(V, M) residues are found in the α1 helix, followed by an amphipathic α2 helix with numerous conserved hydrophobic residues. The α3 helix is characterized by the presence of D(V, I, L) residues. This pattern of sequence conservation is analogous to that seen amongst other histone fold proteins (5, 10, 32). Several metazoan sequences encoding potential proteins with homology to the yTAF$_{II}$47 HFD were also detected in these searches (Fig. 1) (32). This observation indicates that yTAF$_{II}$47 is a histone-like protein belonging to an evolutionarily conserved family. In addition to the α1, α2, and α3 helices, which comprise the minimal HFD, there is a potential additional αC helix in this family.

To determine whether the yTAF$_{II}$47 HFD is important for function, we performed complementation experiments by plasmid shuffle in a yTAF$_{II}$47 null strain. Expression vectors for wild-type or mutated yTAF$_{II}$47 proteins were constructed (Fig. 2A), and their ability to rescue growth of the null strain was evaluated. As previously described, yTAF$_{II}$47 is essential for vegetative yeast growth (34). Expression of full-length yTAF$_{II}$47 efficiently restored the growth of the null strain at 30°C, whereas no growth was seen with the expression vector alone (1 and 3 in Fig. 2B). Growth was also rescued by yTAF$_{II}$47(1–81) containing only the minimal HFD (construct 4 in Fig. 2B). These two strains showed comparable growth rates in liquid culture (data not shown). This 1–81 domain rescued growth both when expressed as a native protein and when expressed as

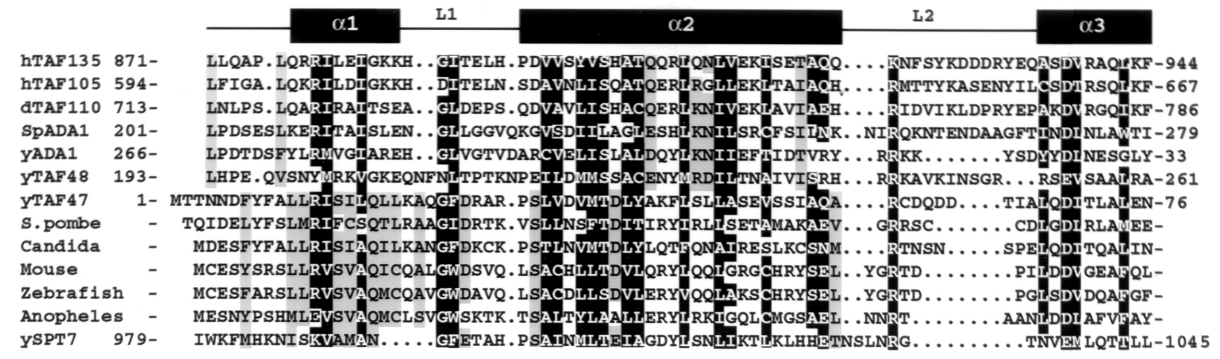

FIG. 1. Alignment of the HFD sequences of the hTAF$_{II}$135 family with those of ADA1 and the yTAF$_{II}$47 family. h, human; y, *Saccharomyces cerevisiae*; d, *Drosophila melanogaster*; S.pombe, *Schizosaccharomyces pombe*; Anopheles, *Anopheles gambiae*; mouse, *Mus musculus*; Candida, *Candida albicans*; zebra fish, *Danio rerio*. The positions of the predicted α helices and loops are indicated above the sequence based on homology with H2A (10, 22). Positions with conserved, mainly hydrophobic, amino acids are in white on a black background. Other residues conserved within the yTAF$_{II}$47 family are boxed in gray. Amino acids were classified as follows: small residues, P, A, G, S, and T; hydrophobic residues, L, I, V, A, F, M, C, Y, and W; polar and/or acidic residues, D, E, Q, and N; basic residues, R, K, and H. Threonine residues are occasionally present in otherwise hydrophobic positions. The amino acids sequences shown without numbers are predicted from genomic, expressed sequence tag, or sequence tagged site sequences. The accession numbers for the indicated sequences are as follows: *S. pombe*, SPT:CAB90151; *Candida*, 396380B03; *Anopheles*, GB CN501GI9 AL143170; zebra fish, GB AW343321fi76b06.y1; mouse, GB AA692266ur52c07.

a fusion with the VP16 activating domain from a two-hybrid expression vector (construct 5 in Fig. 2B). Mutation of the highly conserved amino acids R13 and I14 in the α1 helix (construct m1 in Fig. 2A) abolished the ability of yTAF$_{II}$47(1–81) to rescue growth (construct 6 in Fig. 2B). In contrast, this mutation did not abolish yTAF$_{II}$47 function in the context of the full-length protein (construct 2 in Fig. 2B). The (1–353)m1 mutant did, however, show a temperature-sensitive phenotype, as it did not rescue growth at 37°C while both the wild-type protein and the 1–81 deletion rescued growth at this temperature (compare constructs 1 and 3 in Fig. 2C). The VP16-TAF$_{II}$47(1–81) fusion also showed a temperature-sensitive phenotype (construct 4 in Fig. 2C). These results indicate that the yTAF$_{II}$47 HFD is an essential functional domain necessary and sufficient for vegetative yeast growth.

Genetic interaction between yTAF$_{II}$47 and other histone-like yTAF$_{II}$s. Possible genetic interactions between yTAF$_{II}$47 and other yTAF$_{II}$s were examined. To look for such interactions, we tested the ability of other yTAF$_{II}$s to rescue the temperature-sensitive phenotype of the yTAF$_{II}$47(1–353)m1 allele when overexpressed at the nonpermissive temperature.

The yTAF$_{II}$47(1–353)m1 strain did not grow at 34°C (Fig.

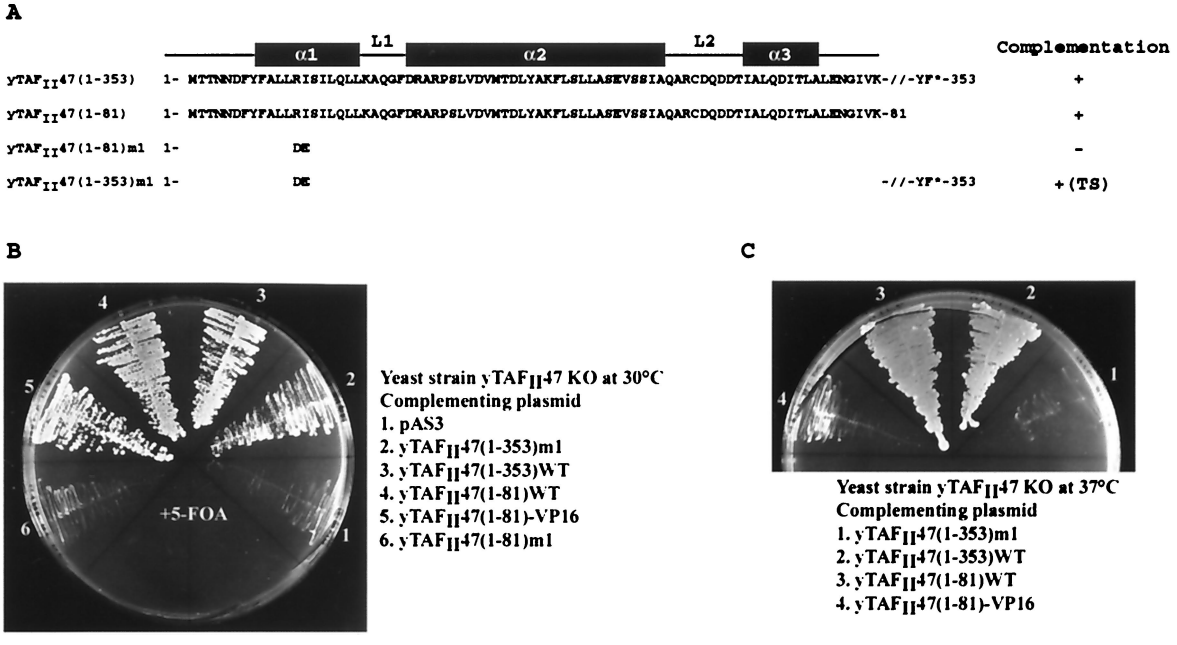

FIG. 2. The yTAF$_{II}$47 HFD is sufficient for growth. (A) The sequence of the yTAF$_{II}$47 HFD is shown along with that of mutant m1. The locations of the potential α helices and loops are indicated above the sequence. The ability of each mutant to complement the null strain is indicated on the right. TS, temperature sensitive. (B and C) Growth of yeasts plated at the indicated temperatures. 5-FOA, 5-fluoroorotic acid.

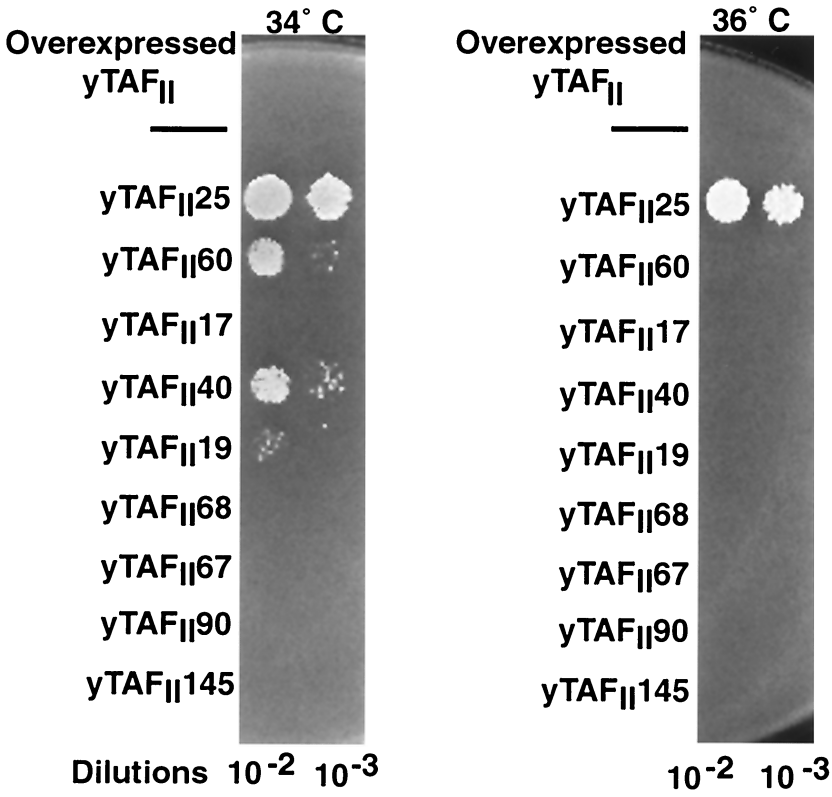

FIG. 3. Genetic interactions among histone-like yTAF$_{II}$s. The growth of serial dilutions of strains with the yTAF$_{II}$47(1–353)m1 allele at 34 and 36°C is shown. The overexpressed yTAF$_{II}$s used to rescue the growth at the nonpermissive temperatures are shown on the left.

3). At 34°C, the temperature-sensitive phenotype was efficiently suppressed by overexpression of yTAF$_{II}$25 and partially suppressed by overexpression of yTAF$_{II}$60, yTAF$_{II}$40, and yTAF$_{II}$19 (Fig. 3). At 36°C, however, only yTAF$_{II}$25 could suppress the temperature-sensitive phenotype (Fig. 3). No significant growth was seen when any of the other yTAF$_{II}$s were overexpressed at either temperature (Fig. 3), while all strains showed equivalent growth at 30°C (data not shown). Analogous results were obtained with the yTAF$_{II}$47(1–81)-VP16 allele (data not shown). These results show a genetic interaction between yTAF$_{II}$47 and three other known histone-like yTAF$_{II}$s, yet the strongest interaction was observed with yTAF$_{II}$25, which has not previously been described as histone-like.

The HFD of yTAF$_{II}$47 mediates heterodimerization with yTAF$_{II}$25. The strong genetic interaction between yTAF$_{II}$47 and yTAF$_{II}$25 prompted us to determine whether they also interact physically. The yTAF$_{II}$47 HFD was fused to the VP16 activation domain or the LexA DNA binding domain and tested for interactions with LexA or VP16 fusions of the core domain of yTAF$_{II}$25 and the HFDs of other yTAF$_{II}$s in a series of yeast two-hybrid experiments. Interactions were assessed by measuring β-galactosidase activity in strain L40, which harbors a LexA-responsive LacZ gene (10, 33).

In two-hybrid assays, a strong interaction between yTAF$_{II}$47 and yTAF$_{II}$25(74–206) was observed (Fig. 4A, column 1). This interaction required only the HFD of yTAF$_{II}$47(1–81) and was abolished by mutation m1 in the α1 helix (Fig. 4A, columns 2 and 3). In the context of the full-length yTAF$_{II}$47, the m1 mutation reduced but did not abolish the interaction (Fig. 4A, column 4). In contrast, we detected no interactions between the HFD of yTAF$_{II}$47 and the HFDs of yTAF$_{II}$40 or yTAF$_{II}$19 (which themselves strongly interact in two-hybrid assays [data not shown]), yTAF$_{II}$60, yTAF$_{II}$68, yTAF$_{II}$48, and yTAF$_{II}$65 (summarized in Table 1). Moreover, we did not observe homodimerization of yTAF$_{II}$47. Similarly, with the exception of yTAF$_{II}$65 (see below), yTAF$_{II}$25 did not interact with the HFDs of the other yTAF$_{II}$s tested (Fig. 4A, columns 5 to 7, and Table 1), although a possible homodimerization was seen

FIG. 4. Selective heterodimerization between yTAF$_{II}$47 and yTAF$_{II}$25 in two-hybrid assays. (A) Quantification of β-galactosidase activity in two-hybrid assays. The VP16-yTAF$_{II}$47, VP16-yTAF$_{II}$40, VP16-yTAF$_{II}$19, and yTAF$_{II}$48 fusions shown below each column were assayed in a LexA-yTAF$_{II}$25(74–206) background as indicated above the graph. β-gal, β -galactosidase. (B) Alignment of yTAF$_{II}$25 and hTAF$_{II}$30 with members of the hTAF$_{II}$28 family from yeast and *D. melanogaster*. Conserved positions are in white against a black background. The positions of the α helices and loops of hTAF$_{II}$28 are indicated. Alignment of the α3 helix of yTAF$_{II}$25 and hTAF$_{II}$30 with that of the other indicated histone fold proteins is also shown. (C) The sequences of the conserved region of yTAF$_{II}$25 and hTAF$_{II}$30 are shown. Conserved amino acids are white on a black background. The end points of the deletions tested in two-hybrid assays are indicated by the arrows below the sequence. Δ, internal deletion. (D) Mapping of the yTAF$_{II}$25 region required for interaction with yTAF$_{II}$47. The LexA-yTAF$_{II}$25 (LexA-hTAF$_{II}$30) deletions indicated below the graph were assayed in the VP16-yTAF$_{II}$47(1–81) strain.

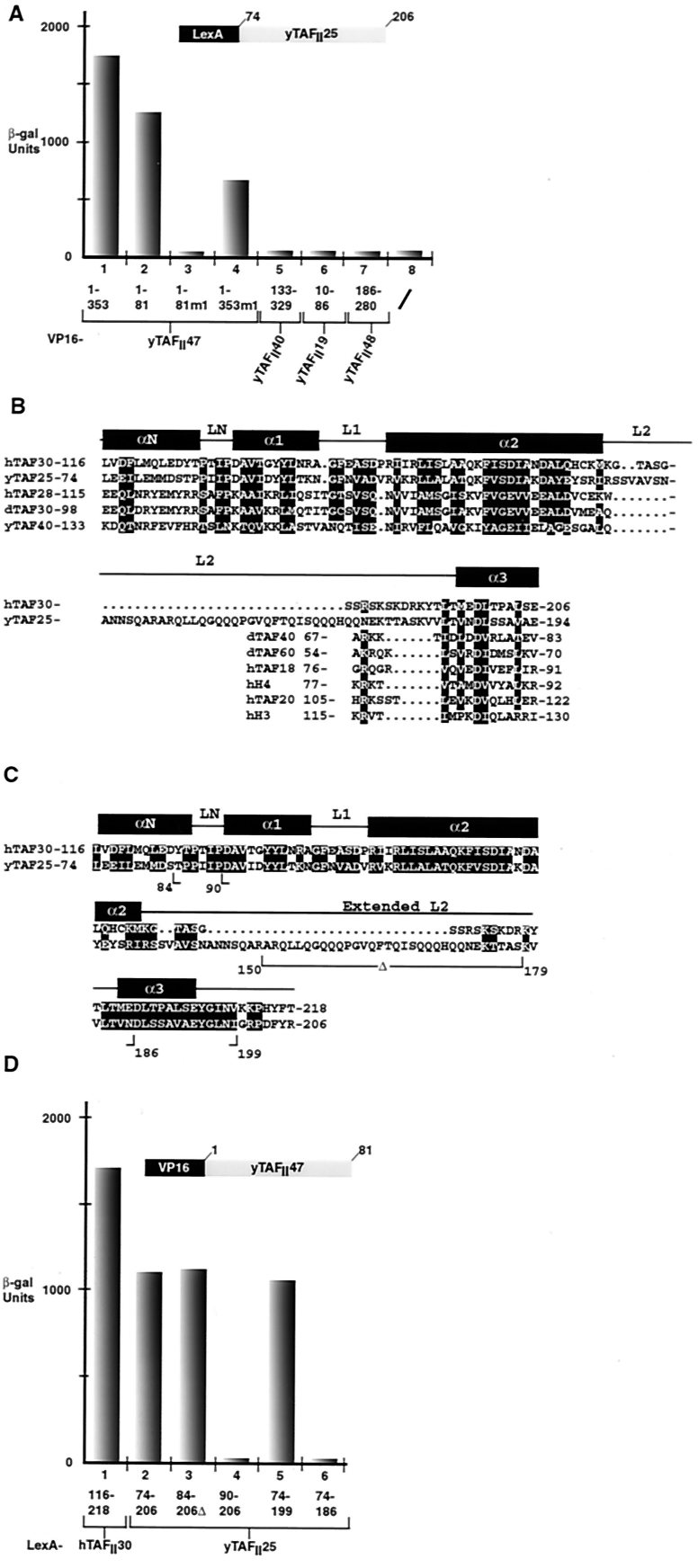
A
2000
β-gal Units
1000
0
LexA
74
206
yTAFII25
1 2 3 4 5 6 7 8
1-353
1-81
1-81m1
1-353m1
133-329
10-86
186-280
VP16-
yTAFII47
yTAFII40
yTAFII19
yTAFII48
B
αN
LN
α1
L1
α2
L2
α3
hTAF30-116
yTAF25-74
hTAF28-115
dTAF30-98
yTAF40-133
hTAF30-
yTAF25-
dTAF40 67-
dTAF60 54-
hTAF18 76-
hH4 77-
hTAF20 105-
hH3 115-
C
84
90
Extended L2
150
179
186
199
D
1
81
VP16
yTAFII47
116-218
74-206
84-206Δ
90-206
74-199
74-186
LexA-
hTAFII30
yTAFII25

TABLE 1. Interactions between TFIID components and various HFDs

Complex	Histone fold	Interaction with HFD[a]							
		TFIID					TFIID + SAGA		
		yTAF$_{II}$47	yTAF$_{II}$48	yTAF$_{II}$65	yTAF$_{II}$40	yTAF$_{II}$19	yTAF$_{II}$25	yTAF$_{II}$68	yTAF$_{II}$60
TFIID	yTAF$_{II}$47	−	−	−	−	−	+++	−	−
	yTAF$_{II}$65	−	−	−	−	−	+++	−	−
TFIID + SAGA	yTAF$_{II}$25	+++	−	+++	−	−	+?	−	ND

[a] −, no interaction; +?, possible homodimerization; +++, strong interaction; ND, not determined.

(Table 1; also, see Discussion). These results indicate that yTAF$_{II}$47 selectively heterodimerizes with yTAF$_{II}$25.

Sequence alignments have shown that hTAF$_{II}$30, yTAF$_{II}$25, and their homologues from other species have a bipartite structure with a highly conserved C-terminal domain and an unconserved N-terminal region (12) (Fig. 4C). In yTAF$_{II}$25, it is the conserved C-terminal region (amino acids 74 to 206) which mediates interaction with the yTAF$_{II}$47 HFD (Fig. 4A and D, column 2). We therefore compared this region of yTAF$_{II}$25 to the other known histone-like TAF$_{II}$s. In doing this, we noted a significant similarity between the sequences of yTAF$_{II}$25/hTAF$_{II}$30 and the HFD of the hTAF$_{II}$28 family of proteins (Fig. 4B). This similarity predicted the existence of potential αN, α1, and α2 helices within yTAF$_{II}$25 and hTAF$_{II}$30, the nonconserved sequence corresponding to an insertion in the L2 loop of yTAF$_{II}$25 (Fig. 4B). In contrast, the proposed α3 helix of yTAF$_{II}$25 contains the conserved D(V, I, L) pair and shows better homology to several other known histone-like proteins than to hTAF$_{II}$28.

We next tested the effect of deleting various regions of the yTAF$_{II}$25 HFD on heterodimerization with yTAF$_{II}$47 (Fig. 4C). Deletion of the αN and a large part of the extended L2 loop [yTAF$_{II}$25(84–206)Δ] had no effect on interaction (Fig. 4D, column 3). However, deletion of the LN led to a loss of interaction despite the fact that the proposed α1 remained in this construct [yTAF$_{II}$25(90–206)] (Fig. 4D, column 4). At the C terminus, interaction with yTAF$_{II}$47 was not affected by deletion up to amino acid 199, leaving intact the proposed α3 helix [yTAF$_{II}$25(74–199)] (Fig. 4D, column 5), whereas interaction was abolished when the α3 was truncated (74–186) (column 6). The conserved C-terminal domain of hTAF$_{II}$30 interacted with yTAF$_{II}$47 as efficiently as yTAF$_{II}$25 [hTAF$_{II}$30 (116–218) and yTAF$_{II}$25(74–206)] (Fig. 4D, columns 1 and 2). Together, these results indicate that the conserved C-terminal domain of the yTAF$_{II}$25 family contains an HFD which heterodimerizes with yTAF$_{II}$47.

To observe direct heterodimerization of yTAF$_{II}$47 and yTAF$_{II}$25, these proteins were coexpressed in *E. coli*. A native version of yTAF$_{II}$25(74–206) or hTAF$_{II}$30(116–218) was coexpressed with a GST fusion of the yTAF$_{II}$47 HFD. When expressed alone, the GST-yTAF$_{II}$47 fusion is largely insoluble and little soluble protein is recovered on the glutathione-Sepharose beads (Fig. 5A, lane 1). In contrast, coexpression with the yTAF$_{II}$25 or hTAF$_{II}$30 HFD solubilizes GST-yTAF$_{II}$47, which is retained in the form of a complex with each of these proteins on the beads (Fig. 5A, lanes 2 and 3). At first, the GST-yTAF$_{II}$47 chimera appears to be more abundant than the untagged yTAF$_{II}$25 or hTAF$_{II}$30 protein. However, the GST moiety of the chimera stains strongly with Coomassie brilliant blue. When this disproportionate staining is taken into account, the yTAF$_{II}$47-yTAF$_{II}$25 ratio would be closer to the 1:1 ratio expected for a heterodimeric complex. This is a selective heterodimerization, since neither solubilization nor complex formation was seen when GST-yTAF$_{II}$47(1–81) was coexpressed with the HFD of yTAF$_{II}$68 (lane 4), previously shown to heterodimerize with yADA1 in this assay (10), yTAF$_{II}$40, or yTAF$_{II}$19 (data not shown). In control experiments, the native yTAF$_{II}$25(74–206) and hTAF$_{II}$30(116–218) proteins were insoluble when expressed alone and were not retained on glutathione beads (Fig. 5D, lanes 4 and 5). These results confirm the direct heterodimerization of the TFIID components yTAF$_{II}$47 and yTAF$_{II}$25, indicating that they form a novel histone-like pair.

Solubilization and complex formation were also observed when GST-yTAF$_{II}$47(1–81) was expressed with yTAF$_{II}$25(74–206)Δ in which the extended L2 loop has been deleted (Fig. 5C, lane 1). A similar result was seen with yTAF$_{II}$25(84–199)Δ, whereas almost no soluble complex was observed with yTAF$_{II}$25 (90–206)Δ (Fig. 5C, lanes 2 and 3). Thus, as observed in the two-hybrid experiments, yTAF$_{II}$47 and yTAF$_{II}$25 heterodimerization does not require the extended L2 loop but does require the LN region.

yTAF$_{II}$65 contains a functional HFD which mediates selective heterodimerization with yTAF$_{II}$25. The above results reveal the presence of considerably more histone fold proteins in TFIID than originally suspected. This prompted us to examined the sequences of other yTAF$_{II}$s for the presence of potential HFDs. Analysis of the novel yTFIID subunit yTAF$_{II}$65 (30) indicates the presence of a potential HFD with similarity to yTAF$_{II}$17/dTAF$_{II}$40/hTAF$_{II}$31 between amino acids 37 and 103 at the N terminus of the protein (Fig. 6A). To determine whether this is a functional domain of the protein, we tested the ability of yTAF$_{II}$65 mutants to complement the growth of the yTAF$_{II}$65 null strain.

Deletions or mutations in the yTAF$_{II}$65 HFD were generated (Fig. 6A and B) and used to complement the yTAF$_{II}$65 null strain. At 30°C, growth was seen with the full-length protein, whereas no growth was seen when the null strain was complemented with yTAF$_{II}$65(1–140) containing only the HFD (Fig. 6C, constructs 2 and 3). Surprisingly, growth at 30°C was also seen using the deletion 103–510, in which the HFD is deleted, and with mutant (1–510)m1, which contains a double amino acid substitution in the α2 helix (Fig. 6C, constructs 4 and 5). These two strains were, however, temperature sensitive, since they did not grow at 37°C, while growth was seen with the wild-type protein (Fig. 6D, constructs 1 to 4). There-

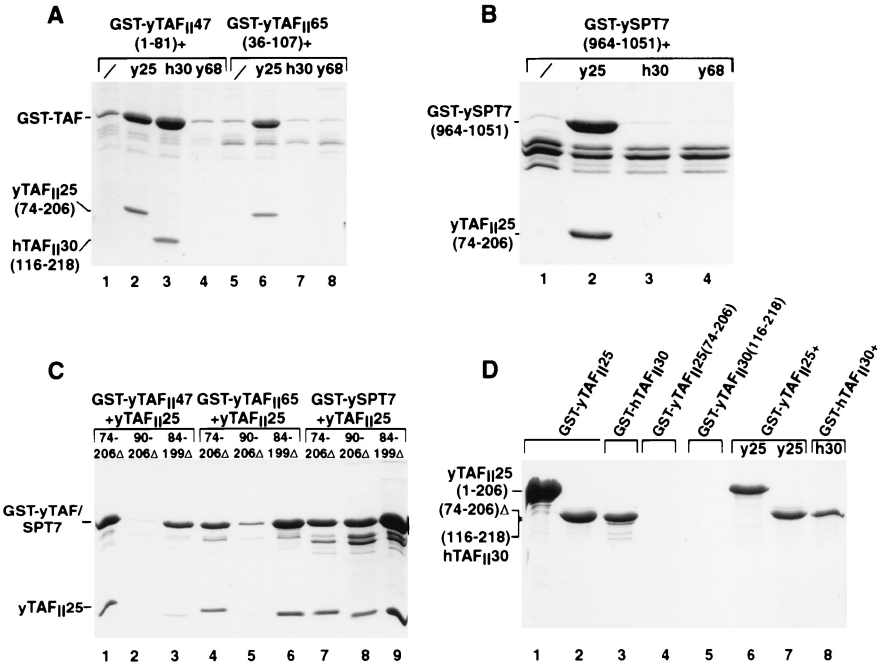

FIG. 5. Coexpression of yTAF$_{II}$47 and yTAF$_{II}$65 with yTAF$_{II}$25 in *E. coli.* (A) Bacteria were transformed to express the proteins shown above each lane. Following extract preparation, the soluble protein retained on glutathione-Sepharose beads was analyzed by sodium dodecyl sulfate-polyacrylamide gel electrophoresis and staining with Coomassie brilliant blue. The locations of the GST-yTAF$_{II}$ fusions and the retained yTAF$_{II}$25 and hTAF$_{II}$30 proteins are indicated. (B) yTAF$_{II}$25-ySPT7 heterodimerization in *E. coli*. The locations of the GST-ySPT7 fusion and yTAF$_{II}$25 are shown. (C) Heterodimerization with yTAF$_{II}$25 deletion mutants. The GST-yTAF$_{II}$47, GST-yTAF$_{II}$65, and GST-SPT7 proteins were coexpressed with the untagged yTAF$_{II}$25 deletion mutants as indicated. The soluble proteins retained on glutathione-Sepharose beads are shown. (D) Lack of evidence for yTAF$_{II}$25 and hTAF$_{II}$30 homodimerization. The GST fusions of yTAF$_{II}$25 and hTAF$_{II}$30 were expressed alone or in combination with the native HFDs indicated above each lane as in panel A.

fore, in contrast to yTAF$_{II}$47, the yTAF$_{II}$65 HFD is not sufficient for vegetative growth. The HFD is nevertheless an important functional domain at 37°C, since its deletion or mutation generates a temperature-sensitive phenotype.

We next tested the ability of yTAF$_{II}$65(1–140) to heterodimerize with the HFDs of other yTAF$_{II}$s in the two-hybrid assay. Surprisingly, a selective interaction was seen only with yTAF$_{II}$25 (Table 1 and Fig. 7B, column 2). Interaction with yTAF$_{II}$25 was seen with full-length yTAF$_{II}$65 (Fig. 7B, column 1), and this interaction was abolished by mutation m1, which also generated a temperature-sensitive phenotype (Fig. 7A, column 4). Interaction with the yTAF$_{II}$65 HFD alone was reduced compared to yTAF$_{II}$65(1–510) or (1–140) [yTAF$_{II}$65(37–107) (Fig. 7A, column 3). Nevertheless, interaction with yTAF$_{II}$25 was totally abolished when two amino acid changes were introduced into the α1 and α2 helices of the yTAF$_{II}$65 HFD [yTAF$_{II}$65(37–103)m2 in Fig. 6A and 7B, column 5]. Interaction with yTAF$_{II}$65 required the conserved C-terminal domain of yTAF$_{II}$25 that was required for interaction with yTAF$_{II}$47 (data not shown). However, in contrast to yTAF$_{II}$47, yTAF$_{II}$65 does not interact with hTAF$_{II}$30 (Fig. 7B, column 6).

As described above for yTAF$_{II}$47, direct yTAF$_{II}$65-yTAF$_{II}$25 heterodimerization was verified by coexpression in *E. coli*. The yTAF$_{II}$65(36–107) HFD was fused to GST and expressed either alone or in combination with the HFD of yTAF$_{II}$25, hTAF$_{II}$30, or yTAF$_{II}$68. As observed for yTAF$_{II}$47, the GST-yTAF$_{II}$65 protein was essentially insoluble when expressed alone, while solubilization and complex formation were observed when GST-yTAF$_{II}$65 was coexpressed with yTAF$_{II}$25(74–206) (Fig. 5A, lanes 5 and 6). In agreement with the two-hybrid assay data, heterodimerization was also observed with yTAF$_{II}$25(74–206)Δ and yTAF$_{II}$25(84–199)Δ but was strongly reduced with (90–206)Δ (Fig. 5C, lanes 4 to 6). Similarly, no complex was formed with the hTAF$_{II}$30 core domain (Fig. 5A, lane 7), and in an additional control no heterodimerization was seen with the yTAF$_{II}$68 HFD (Fig. 5A, lane 8). Therefore, while yTAF$_{II}$47 can heterodimerize with yTAF$_{II}$25 or hTAF$_{II}$30, heterodimerization with yTAF$_{II}$65 is selective for yTAF$_{II}$25 and is not seen with the closely related hTAF$_{II}$30. These results indicate that the TFIID component yTAF$_{II}$65 selectively and directly heterodimerizes with yTAF$_{II}$25 to form an additional histone-like pair.

yTAF$_{II}$25 heterodimerizes with the SAGA component ySPT7. The above results indicate that yTAF$_{II}$25 heterodimerizes with yTAF$_{II}$47 and yTAF$_{II}$65. yTAF$_{II}$25 is present in TFIID and SAGA, yet both yTAF$_{II}$47 and yTAF$_{II}$65 are TFIID specific and are not present in SAGA (29, 30). We therefore sought a potential heterodimerization partner for yTAF$_{II}$25 in the SAGA complex. Database searches with the yTAF$_{II}$47 HFD showed that ySPT7 contains a potential HFD between amino acids 975 and 1051 with similarity to that of yTAF$_{II}$47 (Fig. 1) (32). This observation prompted us to test the ability of the ySPT7 HFD to interact with that of yTAF$_{II}$25. In two-hybrid assays, a strong interaction between ySPT7(964–

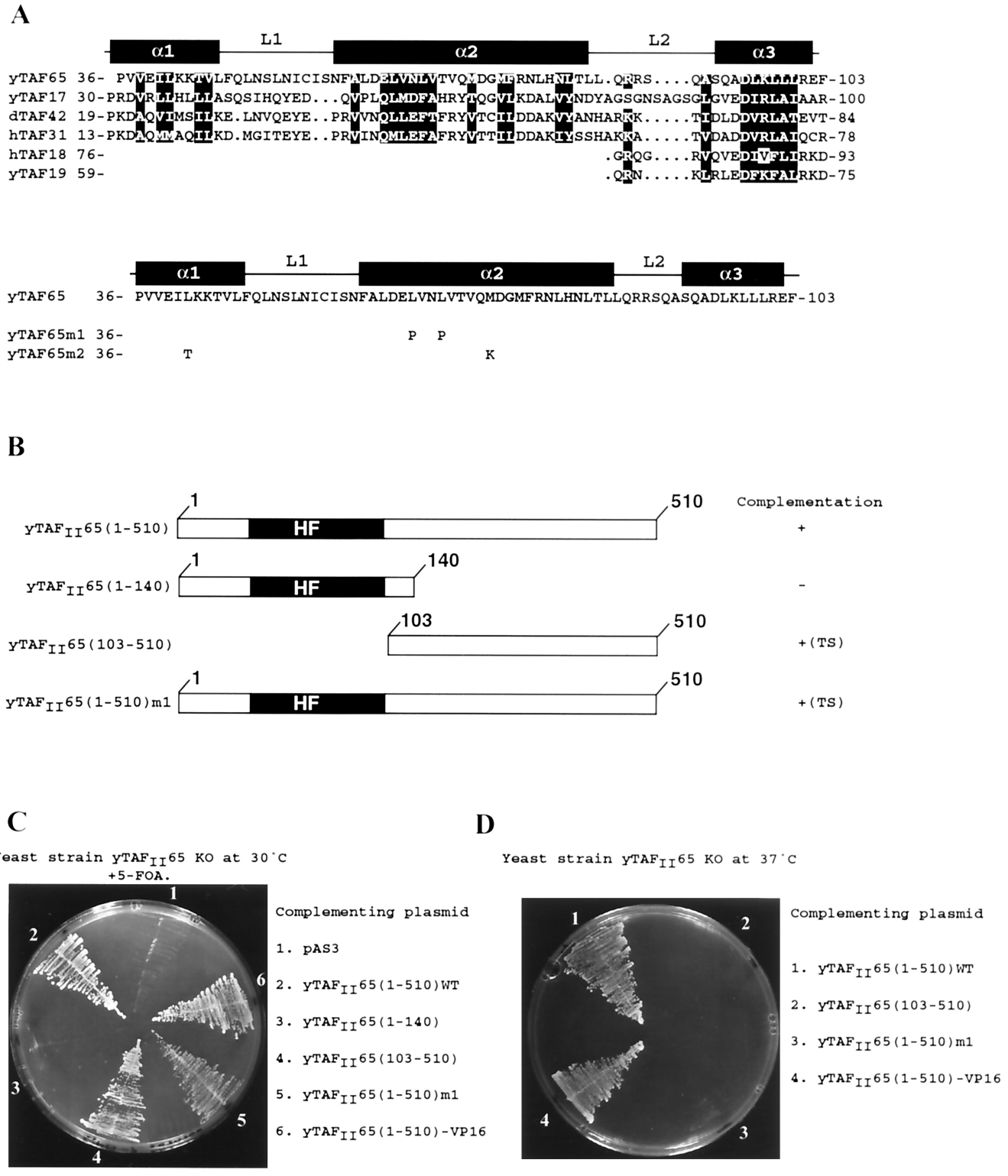

FIG. 6. yTAF$_{II}$65 contains a histone fold motif. The sequence of yTAF$_{II}$65 is aligned with the sequences of members of the yTAF$_{II}$17 family. The conserved positions are white against a black background, and the positions of the α helices and loops are indicated. The sequences of the m1 and m2 mutants are indicated below the wild-type sequence. (B) The structures of the yTAF$_{II}$65 mutants used in complementation experiments are schematized. The HFD is depicted as a black box. TS, temperature sensitive. (C and D) Growth of yeasts plated at the indicated temperatures. 5-FOA, 5-fluoroorotic acid.

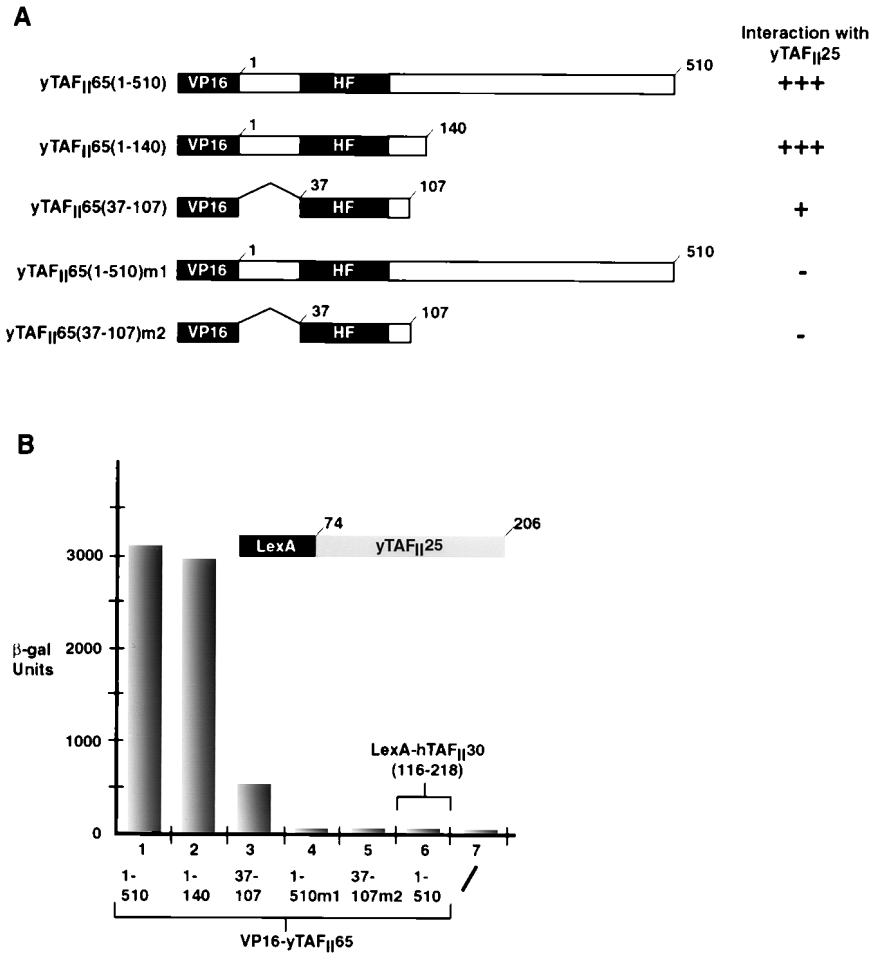

FIG. 7. The histone fold of $yTAF_{II}65$ is required for heterodimerization with $yTAF_{II}25$. (A) Structures of the $yTAF_{II}65$ deletion mutants used in the two-hybrid assays. (B) The VP16-$yTAF_{II}65$ deletions indicated below the graph were assayed in the LexA-$yTAF_{II}25$(74–206) strain. For column 6, $yTAF_{II}65$ was assayed in the LexA-$hTAF_{II}30$(116–218) strain. β-gal, β-galactosidase.

1051) and $yTAF_{II}25$(74–206) was observed (Fig. 8A, column 6, and B, column 1). The $yTAF_{II}25$-ySPT7 two-hybrid interaction was comparable to that seen with both $yTAF_{II}47$ and $yTAF_{II}65$ (Fig. 8A, columns 1, 4, 5, and 6).

Interestingly, the ySPT7 HFD interacted not only with $yTAF_{II}25$(74–206) but also with $yTAF_{II}25$(90–206), which did not interact with either $yTAF_{II}47$ or $yTAF_{II}65$ (Fig. 8B, columns 1 and 2). This indicates that the determinants of $yTAF_{II}25$ required for interaction with ySPT7 are not exactly the same as those required for interaction with $yTAF_{II}47$ and $yTAF_{II}65$. In contrast, ySPT7 did not heterodimerize with $hTAF_{II}30$(116–218) or with the other SAGA components $yTAF_{II}68$ and ADA1, showing that heterodimerization with $yTAF_{II}25$ is highly specific (Fig. 8B, columns 3 to 5).

Heterodimerization between $yTAF_{II}25$ and ySPT7 was verified directly by coexpression in *E. coli*. The GST-ySPT7(964–1051) fusion protein was insoluble when expressed alone, whereas in the presence of $yTAF_{II}25$(74–206) a soluble heterodimeric complex was formed (Fig. 5B, lanes 1 and 2). Therefore, the SAGA components $yTAF_{II}25$ and ySPT7 directly heterodimerize to form a histone-like pair. Consistent with the two-hybrid assay results, no complex was formed with $hTAF_{II}30$(116–218) or with $yTAF_{II}68$ (lanes 3 and 4). In contrast to what was observed with $yTAF_{II}47$ and $yTAF_{II}65$, complex formation with $yTAF_{II}25$(90–206)Δ was as efficient as that with $yTAF_{II}25$(74–206)Δ and $yTAF_{II}25$(84–199)Δ (Fig. 5C, lanes 7 to 9). This is in good agreement with the two-hybrid assay data and confirms that there is a differential requirement for the LN loop in heterodimerization with ySPT7 compared with $yTAF_{II}47$ and $yTAF_{II}65$.

Potential homodimerization of $yTAF_{II}25$. It has previously been reported that both $yTAF_{II}25$ and $hTAF_{II}30$ can interact with themselves (18, 19). Indeed, in our two-hybrid experiments, we observed an interaction between LexA and VP16 fusions of the $yTAF_{II}25$ HFD (Fig. 8A, column 7, and Table 1). We therefore addressed the potential $yTAF_{II}25$ homodimerization in the coexpression assay. In contrast to GST-$yTAF_{II}47$, GST-$yTAF_{II}65$, and GST-ySPT7, both full-length $yTAF_{II}25$ and the $yTAF_{II}25$ ($hTAF_{II}30$) HFD GST fusions were soluble when expressed alone (Fig. 5D, lanes 1 to 3). However, when these GST fusions are coexpressed with the corresponding native HFDs, the untagged HFDs are not retained on the GST-Sepharose beads (Fig. 5D, lanes 6 to 8) as they are when expressed with GST-$yTAF_{II}47$, GST-$yTAF_{II}65$,

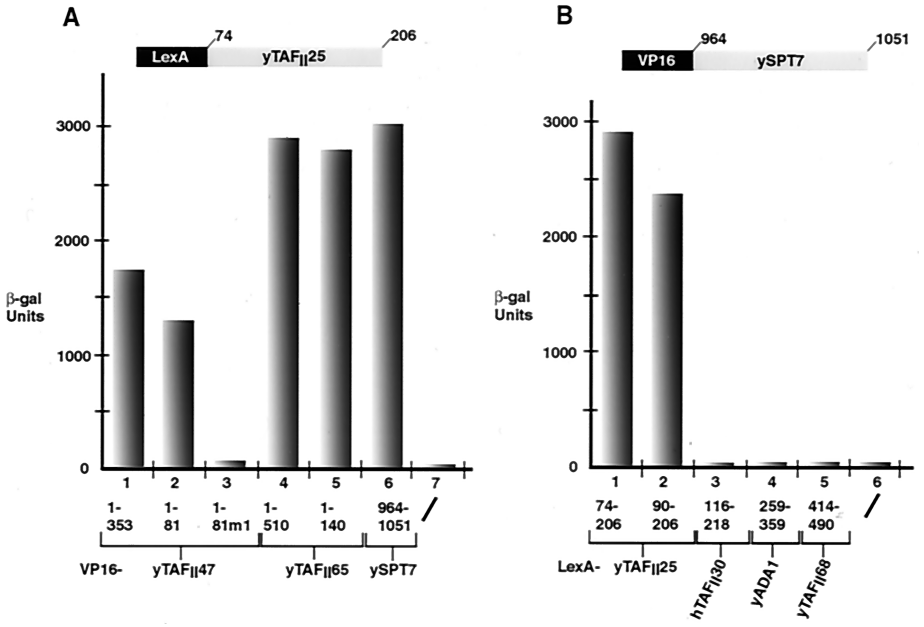

FIG. 8. Heterodimerization of the SAGA components $yTAF_{II}25$ and ySPT7. (A) The VP16 fusions shown below each column were transformed into the LexA-$yTAF_{II}25$(74–206) strain. (B) The LexA fusions shown below each column were transformed into the VP16-SPT7(964–1051) strain. β-gal, β-galactosidase.

or GST-ySPT7. Thus, while we readily observe heterodimerization using this assay, we fail to detect homodimerization of $yTAF_{II}25$ and $hTAF_{II}30$ via their HFDs.

DISCUSSION

Novel histone-like components in TFIID and SAGA. We previously reported that $hTAF_{II}135$ and yADA1 contained HFDs (10). Here we show that $yTAF_{II}47$, $yTAF_{II}25$, and $yTAF_{II}65$ have significant sequence similarities with other TAF_{II}s shown experimentally to contain histone folds. These similarities are comparable to those described for other histone-like proteins (9). Although definitive proof that these are bone fide HFDs will require that their structures be determined, the sequence similarities and the results of our coexpression studies suggest that $yTAF_{II}47$, $yTAF_{II}65$, $yTAF_{II}25$, and ySPT7 are potential histone-like proteins which heterodimerize to form novel pairs in the TFIID and SAGA complexes. Thus, in total there are nine histone-like $yTAF_{II}$s, and the known genetic and physical interactions suggest that they are organized in at least two substructures within TFIID.

Our database searches using the $hTAF_{II}135$ HFD showed the presence of a potential HFD in $yTAF_{II}47$. Further support for this comes from Sullivan et al., who also identified $yTAF_{II}47$ as a histone-like protein using an alternative algorithm (32). The positions of the α helices, notably the α1 helix, proposed by these authors differ significantly from that shown in Fig. 1. This is due mainly to the absence of gaps in the loops in their alignments. Previous alignments of the $hTAF_{II}135$ sequence with that of H2A, whose structure has been determined, favor the alignment shown in Fig. 1A. Furthermore, mutation of the conserved RI pair in $yTAF_{II}47$ abolishes interaction with $yTAF_{II}25$ and the same mutation in $hTAF_{II}135$ abolishes interaction with $hTAF_{II}20$ (our unpublished data). Both observations point to these amino acids being located in the α1 helix, as indicated in our alignments. A definitive assignment of the precise α1 helix boundaries will require that the structure of this molecule be determined. The presence of the highly conserved D(I, V, L) pair allows the position of the α3 helix in each of the proteins described here to be determined based on the alignment with histone fold proteins of known structure.

Interestingly, these database searches reveal the existence of potential metazoan homologues of $yTAF_{II}47$. As the metazoan homologues of $yTAF_{II}25$ ($hTAF_{II}30$ and $dTAF_{II}24/16$) (12, 18) are known TFIID components, it is only to be expected that metazoan TFIID will contain a homologue of their heterodimerization partner, $yTAF_{II}47$. It will be interesting to determine whether the human and mouse proteins revealed in these database searches are TFIID components. These observations reinforce the idea that the structure and function of TFIID have been strongly conserved throughout evolution. Hence, it is likely that metazoan TFIID also contains a homologue of $yTAF_{II}65$ and, as $yTAF_{II}25$ and $hTAF_{II}30$ are components of SAGA, TFTC, and PCAF, we would expect these complexes to contain a homologue of ySPT7.

$yTAF_{II}47$-$yTAF_{II}25$, a novel histone-like pair in yTFIID. Our results show that the $yTAF_{II}47$ HFD is necessary and sufficient for the function of this protein in vivo. The growth of the $yTAF_{II}47$ null strain can be complemented by expression of the HFD alone, and its function is abolished by mutation of the well-conserved RI pair in the α1 helix. Interestingly, this same mutation is not lethal in the context of the full-length protein but rather results in a temperature-sensitive phenotype. One interpretation of this result is that other regions of $yTAF_{II}47$ missing in the 1–81 mutant act to stabilize the interactions of the mutant protein at permissive temperatures. This is also suggested by the observation that heterodimerization with

yTAF$_{II}$25 is abolished by mutation m1 in yTAF$_{II}$47 in the context of the minimal HFD, yet in the context of the full-length yTAF$_{II}$47 mutation m1 does not abolish heterodimerization. It is therefore likely that heterodimerization is necessary for function in vivo. In addition to the three α helices which constitute the minimal HFD, αC and αN helices can often be found. In the yTAF$_{II}$47 family, a short region downstream of the α3 helix is conserved, and computer algorithms predict that this conserved sequence may form an α helix. Therefore, this αC helix or another, as-yet-undefined domain in yTAF$_{II}$47 may act to stabilize interactions with yTAF$_{II}$25 or with other components of yTFIID, but their function becomes evident only when the HFD is mutated.

Our results show that the temperature-sensitive phenotype of the yTAF$_{II}$47(1–353)m1 allele can be suppressed by overexpression of several other histone-like yTAF$_{II}$s. At 34°C, suppression is most efficient with the direct heterodimerization partner yTAF$_{II}$25. A weaker suppression is seen with yTAF$_{II}$40 and yTAF$_{II}$19, suggesting that this pair makes close contact with the yTAF$_{II}$47-yTAF$_{II}$25 pair in native yTFIID. Overexpression of yTAF$_{II}$60, but not its heterodimeric partner yTAF$_{II}$17, can suppress the temperature-sensitive phenotype of this allele, suggesting that this pair may also in some way contact the yTAF$_{II}$47-yTAF$_{II}$25 pair. At higher temperatures, however, only the direct heterodimerization partner yTAF$_{II}$25 can suppress the temperature-sensitive phenotype of the yTAF$_{II}$47(1–353)m1 allele.

We also tested the ability of overexpressed yTAF$_{II}$65 to suppress the TAF$_{II}$47 temperature-sensitive mutation. Interestingly, we found that even at permissive temperatures, yTAF$_{II}$65 overexpression was toxic in the yTAF$_{II}$47 temperature-sensitive background but not in the yTAF$_{II}$47 wild-type or other backgrounds. One interpretation of this result is that at 30°C, the TAF$_{II}$47-TAF$_{II}$25 interaction is already sufficiently weakened that when yTAF$_{II}$65 is overexpressed it competes with yTAF$_{II}$47(1–353)m1 and titrates yTAF$_{II}$25. Consequently, there is no longer enough of the TAF$_{II}$47-TAF$_{II}$25 heterodimer for the yeast to survive, providing evidence that formation of the yTAF$_{II}$47-yTAF$_{II}$25 heterodimer is essential for viability.

In addition to a genetic interaction, our results show that the yTAF$_{II}$47 HFD interacts physically with the conserved C-terminal domain of yTAF$_{II}$25 (and hTAF$_{II}$30) both in yeast two-hybrid assays and by coexpression in *E. coli*. The minimum yTAF$_{II}$25 region necessary for interaction with yTAF$_{II}$47 is located between amino acids 84 and 199. Comparison with the sequences of other families of histone-like TAF$_{II}$s revealed a similarity with the hTAF$_{II}$28 family in the α1-L1-α2 region, but the α3 helix of yTAF$_{II}$25 shows higher homology to those of other known histone fold proteins. Like yTAF$_{II}$40 and ySPT3, yTAF$_{II}$25 contains a large insertion in the L2 loop.

This alignment predicts the existence of a possible αN helix in yTAF$_{II}$25 and hTAF$_{II}$30. The presence of an α helix at this position is also predicted by secondary structure computer algorithms (our unpublished data). Deletion of this helix, however, does not lead to a loss of interaction with yTAF$_{II}$47 or yTAF$_{II}$65. Interestingly, the putative LN loop is highly conserved in the yTAF$_{II}$25/hTAF$_{II}$30 family (12), and its deletion results in a loss of interaction with yTAF$_{II}$47 and yTAF$_{II}$65, but not with ySPT7. This strongly suggests that the LN region plays a critical role in heterodimerization by making direct contacts with yTAF$_{II}$47 and yTAF$_{II}$65 as is seen in the hTAF$_{II}$28-hTAF$_{II}$18 pair (5), while in the yTAF$_{II}$25-ySPT7 heterodimer this interaction either does not take place or is not essential for complex formation.

Introduction of stop codons truncating the α2 helix abolishes yTAF$_{II}$25 function. Moreover, in a screen for yTAF$_{II}$25 temperature-sensitive mutants, several alleles with substitutions at G101 were found (29). This position corresponds to the G residue in the L1 loop, highly conserved in both the yTAF$_{II}$25 and hTAF$_{II}$28 families. A more detailed functional analysis of yTAF$_{II}$25 reveals a tight correlation between its ability to interact with its heterodimerization partners and its function (D. Kirschner and L. Tora, unpublished data).

It has previously been suggested that yTAF$_{II}$25 and hTAF$_{II}$30 may homodimerize (18, 19). Klebanow et al. reported two-hybrid interactions using full-length yTAF$_{II}$25 fusions. Our two-hybrid experiments show that this potential homodimerization requires only the HFD of yTAF$_{II}$25. As it is possible that the two-hybrid interaction is indirect, we wished to visualize homodimerization directly. However, while the GST-yTAF$_{II}$25 (74–206) fusion was relatively soluble in *E. coli* when expressed alone, no homodimerization was seen when it was coexpressed with native yTAF$_{II}$25(74–206). Therefore, under the conditions used to observe heterodimerization via the HFD, we detected no yTAF$_{II}$25 homodimerization. Consequently, it is unlikely that the observed yTAF$_{II}$25 oligomerization represents the formation of a histone-like homodimer. This does not, however, exclude the possibility that oligomerization of yTAF$_{II}$25 may occur in some other way, involving for example loop-loop interactions or via the exposed hydrophilic faces of the α helices.

yTAF$_{II}$65-yTAF$_{II}$25, a novel histone-like pair in yTFIID. Here we have identified an HFD in the N terminus of yTAF$_{II}$65. This HFD shows high homology to the yTAF$_{II}$17/hTAF$_{II}$31 family. Both two-hybrid analysis and coexpression in *E. coli* indicate that the yTAF$_{II}$65 HFD mediates a selective heterodimerization with the same yTAF$_{II}$25 domain that is required for interaction with yTAF$_{II}$47. The yTAF$_{II}$65 HFD alone is sufficient to allow interaction with yTAF$_{II}$25, and interaction is abolished by mutations within this domain. These results strongly suggest that yTAF$_{II}$25-yTAF$_{II}$65 form an additional histone-like pair in TFIID. Unlike yTAF$_{II}$47, yTAF$_{II}$65 does not interact with the hTAF$_{II}$30 HFD despite their high homology. We have previously reported that hTAF$_{II}$20, but not yTAF$_{II}$68, interacts with hTAF$_{II}$135. In this case, an important determinant for specificity was mapped to the L2-α3 region of the hTAF$_{II}$20/yTAF$_{II}$68 HFD (10). This observation together with those reported here indicate that there is a strict specificity code which determines the choice of a heterodimerization partner.

The yTAF$_{II}$65 HFD is not sufficient for growth and in fact is not essential at 30°C. Nevertheless, the yTAF$_{II}$65 HFD contributes to function, since its deletion or mutation results in a temperature-sensitive phenotype. It has previously been shown that introduction of proline residues in the α2 helix of yTAF$_{II}$60 and yTAF$_{II}$17 results in a temperature-sensitive phenotype (24). This is also true for yTAF$_{II}$65, since the m1 mutation which introduces two prolines generates a temperature-sensitive phenotype. This same mutant abolishes interaction with yTAF$_{II}$25. In yTAF$_{II}$47 and yTAF$_{II}$68 the HFD is necessary and sufficient for growth. In contrast, however, yTAF$_{II}$65

must contain another essential domain(s) located between amino acids 103 and 510. Further complementation analysis reveals that this essential domain(s) is located between amino acids 161 and 406 (our unpublished data). In this context, it is interesting that, as with yTAF$_{II}$47, we attempted to suppress the temperature-sensitive phenotype of this mutation by overexpression of other yTAF$_{II}$s. In this case, however, the only genetic interaction detected was with yTAF$_{II}$68, whose overexpression suppressed the temperature-sensitive phenotype not only of yTAF$_{II}$65(1–510)m1 but also of yTAF$_{II}$65(103–510), in which the HFD is deleted (our unpublished data). There is therefore a genetic interaction between yTAF$_{II}$68 and yTAF$_{II}$65, but this involves a functional domain(s) of yTAF$_{II}$65 other than the HFD.

yTAF$_{II}$25-ySPT7 a novel histone-like pair in ySAGA. We have shown here that yTAF$_{II}$25 can heterodimerize with yTAF$_{II}$47 and yTAF$_{II}$65. Both of these heterodimerization partners are TFIID specific and are not present in SAGA. yTAF$_{II}$25 is, however, a SAGA subunit, and therefore, an additional heterodimerization partner for yTAF$_{II}$25 must exist in this complex. Our results, and those of Sullivan et al. (32), identified an HFD in ySPT7, and we show that this HFD heterodimerizes with the yTAF$_{II}$25 HFD in both the two-hybrid and bacterial coexpression assays. This HFD is found in the C-terminal half of the protein, which has been reported to partially rescue the phenotype of the SPT7 null strain (11). Genetic studies have also shown that mutations in SPT7 have the same severe phenotype as mutations in ADA1 and SPT20. Mutation of each of these proteins completely disrupts the SAGA complex, showing that they are critical for its structural integrity (31). We have previously reported a direct interaction between the TAF$_{II}$ and ADA families of proteins through the heterodimerization of yTAF$_{II}$68 with yADA1 (10). Here we show that the histone fold is also the interface between the TAF$_{II}$ and the SPT families in SAGA. Together with the genetic studies, this suggests that the yTAF$_{II}$68-yADA1 and yTAF$_{II}$25-SPT7 pairs are both key structural elements of SAGA.

Implications for TFIID structure. In summary, our present results show yTFIID to comprise at least nine histone-like yTAF$_{II}$s rather than the three originally described. These yTAF$_{II}$s assemble into five heterodimeric pairs (yTAF$_{II}$60-yTAF$_{II}$17, yTAF$_{II}$40-yTAF$_{II}$19, yTAF$_{II}$68-yTAF$_{II}$48, yTAF$_{II}$25-yTAF$_{II}$47, and yTAF$_{II}$25-yTAF$_{II}$65). Amongst these, yTAF$_{II}$25 appears to be a key player which can form two distinct heterodimers in TFIID. Previous results have indicated that yTAF$_{II}$47 can be coimmunoprecipitated with yTAF$_{II}$65 in extracts from yeast strains harboring an epitope-tagged yTAF$_{II}$65 (30). This excludes the possibility that the yTAF$_{II}$25-yTAF$_{II}$47 and yTAF$_{II}$25-yTAF$_{II}$65 pairs are present in distinct populations of yTFIID complexes; instead, it indicates that the two pairs coexist in the same population of yTFIID.

It has previously been shown that a temperature-sensitive allele of yTAF$_{II}$17 can be suppressed by overexpression of yTAF$_{II}$60 or yTAF$_{II}$68 and that a temperature-sensitive allele of yTAF$_{II}$60 can be suppressed by overexpressed yTAF$_{II}$17 and yTAF$_{II}$68 (24). Furthermore, yTAF$_{II}$48 overexpression can suppress a temperature-sensitive mutant of yTAF$_{II}$68 (28). These genetic interactions were interpreted as providing evidence of an octamer-like substructure in TFIID (24). Our present results showing genetic interactions between yTAF$_{II}$47 and yTAF$_{II}$25, yTAF$_{II}$40, yTAF$_{II}$19, and yTAF$_{II}$60 suggest a more complex picture which is difficult to interpret in the context of a single octamer-like substructure. Altogether, the existing data suggest that there may be at least two potential substructures, one composed of yTAF$_{II}$68, yTAF$_{II}$60, yTAF$_{II}$48, and yTAF$_{II}$17 as described by Michel et al. and Reese et al. (24, 28) and the other composed minimally of yTAF$_{II}$47, yTAF$_{II}$40, yTAF$_{II}$25, and yTAF$_{II}$19 as reported here. The suppression of the yTAF$_{II}$47 temperature-sensitive allele by overexpressed yTAF$_{II}$60 further implies interplay between the substructures via yTAF$_{II}$60. The stoichiometry of the yTAF$_{II}$s present within each substructure and whether they interact in a way analogous to the core histones in the nucleosome octamer remain to be determined. Similarly, it is not clear whether the yTAF$_{II}$25-yTAF$_{II}$65 pair associates with the yTAF$_{II}$25-yTAF$_{II}$47 substructure via the yTAF$_{II}$25-yTAF$_{II}$25 interactions discussed above or whether it is located elsewhere within TFIID.

ACKNOWLEDGMENTS

We thank S. Hollenberg for the generous gift of yeast strain L40, L. Carré for technical assistance, S. Thuault for gifts of material and critical comments, S. Werten for gifts of materials, S. Vicaire and D. Stephane for DNA sequencing, the staff of cell culture and oligonucleotide facilities, and B. Boulay and J. M. Lafontaine for illustrations.

C.R. was supported by EMBO fellowships. This work was supported by grants from the CNRS, the INSERM, the Hôpital Universitaire de Strasbourg, the Ministère de la Recherche et de la Technologie, the Association pour la Recherche contre le Cancer, the Ligue Nationale contre le Cancer, the Human Frontier Science Programme, and NIH grant GM52461.

REFERENCES

1. **Andel, F., III, A. G. Ladurner, C. Inouye, R. Tjian, and E. Nogales.** 1999. Three-dimensional structure of the human TFIID-IIA-IIB complex. Science **286:**2153–2156.
2. **Apone, L. M., C. A. Virbasius, F. C. Holstege, J. Wang, R. A. Young, and M. R. Green.** 1998. Broad, but not universal, transcriptional requirement for yTAF$_{II}$17, a histone H3-like TAF$_{II}$ present in TFIID and SAGA. Mol. Cell **2:**653–661.
3. **Apone, L. M., C. M. Virbasius, J. C. Reese, and M. R. Green.** 1996. Yeast TAF$_{II}$90 is required for cell-cycle progression through G2/M but not for general transcription activation. Genes Dev. **10:**2368–2380.
4. **Bell, B., and L. Tora.** 1999. Regulation of gene expression by multiple forms of TFIID and other novel TAF$_{II}$-containing complexes. Exp. Cell Res. **246:** 11–19.
5. **Birck, C., O. Poch, C. Romier, M. Ruff, G. Mengus, A. C. Lavigne, I. Davidson, and D. Moras.** 1998. Human TAF$_{II}$28 and TAF$_{II}$18 interact through a histone fold encoded by atypical evolutionary conserved motifs also found in the SPT3 family. Cell **94:**239–249.
6. **Brand, M., C. Leurent, V. Mallouh, L. Tora, and P. Schultz.** 1999. Three-dimensional structures of the TAF$_{II}$-containing complexes TFIID and TFTC. Science **286:**2151–2153.
7. **Brand, M., K. Yamamoto, A. Staub, and L. Tora.** 1999. Identification of TATA-binding protein-free TAF$_{II}$-containing complex subunits suggests a role in nucleosome acetylation and signal transduction. J. Biol. Chem. **274:** 18285–18289.
8. **Burley, S. K., and R. G. Roeder.** 1996. Biochemistry and structural biology of transcription factor IID (TFIID). Annu. Rev. Biochem. **65:**769–799.
9. **Burley, S. K., X. Xie, K. L. Clark, and F. Shu.** 1997. Histone-like transcription factors in eukaryotes. Curr. Opin. Struct. Biol. **7:**94–102.

9a. **Fribourg, S., C. Romier, S. Werten, Y. G. Gangloff, A. Poterszman, and D. Moras.** Dissecting the interaction network of multiprotein complexes by pairwise coexpression of subunits in E. coli. J. Mol. Biol., in press.

10. **Gangloff, Y. G., S. Werten, C. Romier, L. Carre, O. Poch, D. Moras, and I. Davidson.** 2000. The human TFIID components TAF$_{II}$135 and TAF$_{II}$20 and the yeast SAGA components ADA1 and TAF$_{II}$68 heterodimerize to form histone-like pairs. Mol. Cell. Biol. **20:**340–351.
11. **Gansheroff, L. J., C. Dollard, P. Tan, and F. Winston.** 1995. The Saccharomyces cerevisiae SPT7 gene encodes a very acidic protein important for transcription in vivo. Genetics **139:**523–536.
12. **Georgieva, S., D. B. Kirschner, T. Jagla, E. Nabirochkina, S. Hanke, H.**

Schenkel, C. de Lorenzo, P. Sinha, K. Jagla, B. Mechler, and L. Tora. 2000. Two novel *Drosophila* TAF_{II}s have homology with human $TAF_{II}30$ and are differentially regulated during development. Mol. Cell. Biol. **20:**1639–1648.

13. **Grant, P. A., D. Schieltz, M. G. Pray-Grant, D. J. Steger, J. C. Reese, J. R. Yates, and J. L. Workman.** 1998. A subset of TAF_{II}s are integral components of the SAGA complex required for nucleosome acetylation and transcriptional stimulation. Cell **94:**45–53.
14. **Green, M. R.** 2000. TBP-associated factors (TAF_{II}s): multiple, selective transcriptional mediators in common complexes. Trends Biochem. Sci. **25:** 59–63.
15. **Hampsey, M.** 1998. Molecular genetics of the RNA polymerase II general transcriptional machinery. Microbiol. Mol. Biol. Rev. **62:**465–503.
16. **Hoffmann, A., T. Oelgeschlager, and R. G. Roeder.** 1997. Considerations of transcriptional control mechanisms: do TFIID-core promoter complexes recapitulate nucleosome-like functions? Proc. Natl. Acad. Sci. USA **94:**8928–8935.
17. **Hoffmann, A., and R. G. Roeder.** 1996. Cloning and characterization of human TAF20/15. Multiple interactions suggest a central role in TFIID complex formation. J. Biol. Chem. **271:**18194–18202.
18. **Jacq, X., C. Brou, Y. Lutz, I. Davidson, P. Chambon, and L. Tora.** 1994. Human $TAF_{II}30$ is present in a distinct TFIID complex and is required for transcriptional activation by the estrogen receptor. Cell **79:**107–117.
19. **Klebanow, E. R., D. Poon, S. Zhou, and P. A. Weil.** 1996. Isolation and characterization of TAF25, an essential yeast gene that encodes an RNA polymerase II-specific TATA-binding protein-associated factor. J. Biol. Chem. **271:**13706–13715.
20. **Kokubo, T., D. W. Gong, J. C. Wootton, M. Horikoshi, R. G. Roeder, and Y. Nakatani.** 1994. Molecular cloning of Drosophila TFIID subunits. Nature **367:**484–487.
21. **Komarnitsky, P. B., B. Michel, and S. Buratowski.** 1999. TFIID-specific yeast TAF40 is essential for the majority of RNA polymerase II-mediated transcription in vivo. Genes Dev. **13:**2484–2489.
22. **Luger, K., A. W. Mader, R. K. Richmond, D. F. Sargent, and T. J. Richmond.** 1997. Crystal structure of the nucleosome core particle at 2.8 A resolution. Nature **389:**251–260.
23. **Martinez, E., T. K. Kundu, J. Fu, and R. G. Roeder.** 1998. A human SPT3-TAFII31-GCN5-L acetylase complex distinct from transcription factor IID. J. Biol. Chem. **273:**23781–23785.
24. **Michel, B., P. Komarnitsky, and S. Buratowski.** 1998. Histone-like TAFs are essential for transcription in vivo. Mol. Cell **2:**663–673.
25. **Moqtaderi, Z., M. Keaveney, and K. Struhl.** 1998. The histone H3-like TAF is broadly required for transcription in yeast. Mol. Cell **2:**675–682.
26. **Natarajan, K., B. M. Jackson, E. Rhee, and A. G. Hinnebusch.** 1998. $yTAF_{II}61$ has a general role in RNA polymerase II transcription and is required by Gcn4p to recruit the SAGA coactivator complex. Mol. Cell **2:**683–692.
27. **Ogryzko, V. V., T. Kotani, X. Zhang, R. L. Schlitz, T. Howard, X. J. Yang, B. H. Howard, J. Qin, and Y. Nakatani.** 1998. Histone-like TAFs within the PCAF histone acetylase complex. Cell **94:**35–44.
28. **Reese, J. C., Z. Zhang, and H. Kurpad.** 2000. Identification of a yeast transcription factor IID subunit, TSG2/TAF48. J. Biol. Chem. **275:**17391–17398.
29. **Sanders, S. L., E. R. Klebanow, and P. A. Weil.** 1999. TAF25p, a non-histone-like subunit of TFIID and SAGA complexes, is essential for total mRNA gene transcription in vivo. J. Biol. Chem. **274:**18847–18850.
30. **Sanders, S. L., and P. A. Weil.** 2000. Identification of two novel TAF subunits of the yeast Saccharomyces cerevisiae TFIID complex. J. Biol. Chem. **275:** 13895–13900.
31. **Sterner, D. E., P. A. Grant, S. M. Roberts, L. J. Duggan, R. Belotserkovskaya, L. A. Pacella, F. Winston, J. L. Workman, and S. L. Berger.** 1999. Functional organization of the yeast SAGA complex: distinct components involved in structural integrity, nucleosome acetylation, and TATA-binding protein interaction. Mol. Cell. Biol. **19:**86–98.
32. **Sullivan, S. A., L. Aravind, I. Makalowska, A. D. Baxevanis, and D. Landsman.** 2000. The histone database: a comprehensive WWW resource for histones and histone fold-containing proteins. Nucleic Acids Res **28:**320–322.
33. **vom Baur, E., C. Zechel, D. Heery, M. J. Heine, J. M. Garnier, V. Vivat, B. Le Douarin, H. Gronemeyer, P. Chambon, and R. Losson.** 1996. Differential ligand-dependent interactions between the AF-2 activating domain of nuclear receptors and the putative transcriptional intermediary factors mSUG1 and TIF1. EMBO J. **15:**110–124.
34. **Walker, S. S., J. C. Reese, L. M. Apone, and M. R. Green.** 1996. Transcription activation in cells lacking $TAF_{II}S$. Nature **383:**185–188.
35. **Walker, S. S., W. C. Shen, J. C. Reese, L. M. Apone, and M. R. Green.** 1997. Yeast $TAF_{II}145$ required for transcription of G1/S cyclin genes and regulated by the cellular growth state. Cell **90:**607–614.
36. **Wieczorek, E., M. Brand, X. Jacq, and L. Tora.** 1998. Function of TAF_{II}-containing complex without TBP in transcription by RNA polymerase II. Nature **393:**187–191.
37. **Xie, X., T. Kokubo, S. L. Cohen, U. A. Mirza, A. Hoffmann, B. T. Chait, R. G. Roeder, Y. Nakatani, and S. K. Burley.** 1996. Structural similarity between TAFs and the heterotetrameric core of the histone octamer. Nature **380:** 316–322.